J. Fluid Mech. (1981), *vol.* 112, *pp.* 151–160
Printed in Great Britain

Transition from shear to sideways diffusive instability in a vertical slot

By SIVAGNANAM THANGAM,† ABDELFATTAH ZEBIB AND C. F. CHEN‡

Department of Mechanical and Aerospace Engineering, Rutgers University, New Brunswick, New Jersey 08903, U.S.A.

(Received 7 July 1980 and in revised form 13 May 1981)

Stability of the steady motion of a fluid confined between two differentially heated rigid vertical plates is considered. When a stable, constant vertical salinity gradient is also present, the steady mean velocity in the vertical direction and the mean lateral salinity gradient are characterized by the solute Rayleigh number, R_s. Experimental investigations (Elder 1965; Hart 1970) show that when $R_s = 0$ the instability is induced by shear and occurs in the form of two-dimensional convection cells. However, at moderate values of R_s, these shear instabilities are replaced by double-diffusive cellular convection (Thorpe, Hutt & Soulsby 1969; Paliwal & Chen 1980*a*). It is generally believed that the instability is stationary and cellular for all values of R_s (Hart 1971; Paliwal & Chen 1980*b*). We have solved the general eigenvalue problem, and our results indicate that, during transition from the stationary shear-induced instability to stationary double-diffusive cellular convection, overstable motion occurs. Furthermore, in this transition region, over a range of moderately small values of R_s, there is no preferred wavelength at the onset of instability.

1. Introduction

Instability of a fluid layer bounded by two rigid differentially heated vertical plates has been the subject of considerable interest. Elder (1965) and Hart (1970) carried out experimental and theoretical investigations to study the onset of instability in a homogeneous fluid with lateral and vertical temperature gradients. For the case when the vertical temperature gradient is negligible, if the temperature of one of the walls is raised slowly, the lateral temperature gradient will remain constant, and the isotherms would be parallel to the side walls. Their results show that at the onset of instability, induced purely by shear, stationary two-dimensional rolls are formed.

Another interesting phenomenon, the thermosolutal instability, occurs when a stable constant vertical salinity gradient is present in the fluid. The isohalines tend to become parallel with an upward slant towards the heated wall, except in the region near the walls where these lines are horizontal owing to the non-diffusive nature of the boundaries involved. In the interior region there may not be any net horizontal density gradient. However, any small lateral displacement of the fluid could lead to destabilization because of the difference in the diffusivity between heat

† Present address: Stevens Institute of Technology, Hoboken, New Jersey 07030.
‡ Present address: The University of Arizona, Tucson, Arizona 85721.

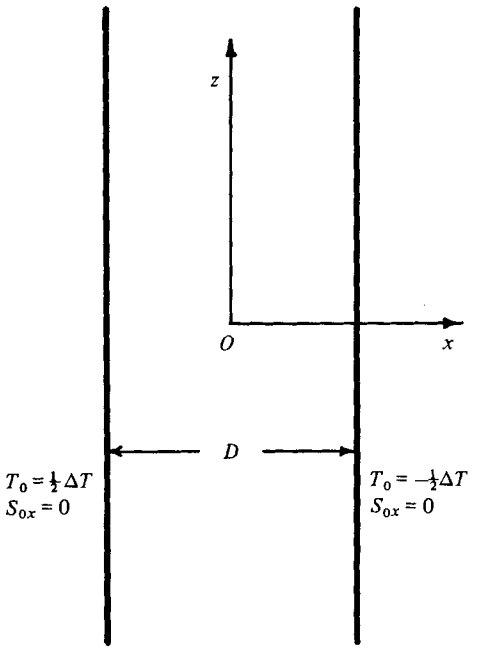

FIGURE 1. The co-ordinate system.

and the solute. Experimental investigations by Thorpe *et al.* (1969), and Paliwal & Chen (1980*a*) indicate that, at moderately large values of the solute Rayleigh number, R_s (defined in § 2), the instability manifests itself in the form of stationary two-dimensional rolls. Based on this, Hart (1971) and Paliwal & Chen (1980*b*) carried out linear stability analyses to study the transition from the shear-induced thermal instability to the double-diffusive thermosolutal instability. To obtain the neutral stability curves, they assumed that only stationary two-dimensional rolls are possible for all values of R_s.

In this paper, we propose to show that, even though the instability occurs in the form of stationary two-dimensional convection cells at very small and at moderately large values of R_s, there are ranges in the values of R_s, where the motion is overstable at the onset of instability. Also, for yet other values of R_s, stationary convection sets in with no preferred wavelength.

2. Formulation

We consider an incompressible fluid layer bounded by two differentially heated rigid parallel plates separated by a distance D. The co-ordinate system is shown in figure 1. There is a constant salinity gradient, $\Phi_0 = dS_0^*/dz^*$ in the vertical direction. The boundaries are considered to be non-diffusive to salt and perfectly heat conducting with a temperature difference ΔT across them. The temperature gradient is constant in the lateral direction. For small variations in temperature and solute concentration, the equation of state can be written as

$$\rho^* = \rho_r[1-\beta_t(T^*-T_r^*)+\beta_s(S^*-S_r^*)] \tag{2.1}$$

where

$$\beta_t^* = -\frac{1}{\rho_r^*}\left(\frac{\partial \rho^*}{\partial T^*}\right)_{S^*P^*}$$

is the coefficient of thermal expansion and

$$\beta_s^* = \frac{1}{\rho_r^*}\left(\frac{\partial \rho^*}{\partial S^*}\right)_{T^*P^*}$$

is the coefficient of volumetric expansion. The subscript r indicates a suitable reference state and an asterisk indicates that the quantities are in dimensional form. Temperature, salinity, pressure and density are respectively represented by T, S, P and ρ.

The equations of continuity, momentum, and the transport equations of heat and solute for an incompressible fluid with Boussinesq approximation are

$$\nabla . \mathbf{u}^* = 0, \tag{2.2}$$

$$\frac{D\mathbf{u}^*}{D\tau^*} = -\frac{1}{\rho_r^*}\nabla P^* + \nu \nabla^2 \mathbf{u}^* - [\beta_t(T^* - T_r^*) - \beta_s(S^* - S_r^*)]\,\mathbf{g}^*, \tag{2.3}$$

$$\frac{DT^*}{D\tau^*} = \kappa_t \nabla^2 T^*, \tag{2.4}$$

$$\frac{DS^*}{D\tau^*} = \kappa_s \nabla^2 S^*. \tag{2.5}$$

In this set of equations, $\mathbf{u}^* = \{u^*, v^*, w^*\}$ is the velocity, $\mathbf{g}^* = \{0, 0, g\}$ is the acceleration due to gravity, and τ is time. The thermal diffusivity, the solute diffusivity and the kinematic viscosity are respectively represented by κ_t, κ_s and ν.

The boundary conditions are

$$T^* = \pm \tfrac{1}{2}\Delta T, \quad S_x^* = 0, \quad u^* = v^* = w^* = 0 \quad \text{at} \quad x^* = \mp \tfrac{1}{2}D. \tag{2.6}$$

The pressure term in equation (2.3) is eliminated by cross-differentiation and (2.3)–(2.5) are made dimensionless with the scaling parameters D for length, D^2/κ_t for time, ΔT for temperature and $D|\Phi_0|$ for solute concentration. We further consider the motion to be two-dimensional in the x, z plane. The governing equations are

$$\left[\frac{1}{Pr}(\partial_\tau + u\partial_x + w\partial_z)(\partial_{xx} + \partial_{zz}) - (\partial_{xx} + \partial_{zz})^2\right]\Psi - (R_t \partial_x T - R_s \partial_x S) = 0, \tag{2.7}$$

$$[\partial_\tau + u\partial_x + w\partial_z - (\partial_{xx} + \partial_{zz})]\,T = 0, \tag{2.8}$$

$$[\partial_\tau + u\partial_x + w\partial_z - Le(\partial_{xx} + \partial_{zz})]\,S = 0, \tag{2.9}$$

where Ψ is the dimensionless stream function defined such that it satisfies $w = \Psi_x$ and $u = -\Psi_z$, $R_t = g\beta_t \Delta T D^3/\kappa_t \nu$ is the thermal Rayleigh number, $R_s = g\beta_s|\Phi_0|\,D^4/\kappa_t \nu$ is the solute Rayleigh number, $Pr = \nu/\kappa_t$ is the Prandtl number, and $Le = \kappa_s/\kappa_t$ is the Lewis number.

The equations describing the stable steady state are obtained from (2.7)–(2.9), by assuming that the velocity is invariant in the z direction, and that the lateral velocity component is zero. The equations are

$$W_{0xxx} + R_t T_{0x} - R_s S_{0x} = 0, \tag{2.10}$$

$$T_{0xx} = 0, \tag{2.11}$$

$$S_{0xx} + \frac{1}{Le} W_0 = 0, \tag{2.12}$$

with the boundary conditions

$$W_0 = S_{0x} = 0, \quad T_0 = \pm \tfrac{1}{2} \quad \text{at} \quad x = \mp \tfrac{1}{2}. \tag{2.13}$$

The solution of (2.10)–(2.12) is

$$W_0 = \frac{R_t}{2M^3(\sin M + \sinh M)} (\sinh M_1 \sin M_2 - \sin M_1 \sinh M_2), \tag{2.14}$$

$$T_0 = -x, \tag{2.15}$$

$$S_{0x} = -\frac{R_t}{4\,Le\,M^4}\left[1 + \frac{1}{\sin M + \sinh M} (\cosh M_1 \sin M_2 - \cosh M_2 \sin M_1 - \sinh M_1 \cos M_2 + \sinh M_2 \cos M_1)\right] \tag{2.16}$$

where

$$M = \left(\frac{R_s}{4\,Le}\right)^{\frac{1}{4}}, \quad M_1 = \left(Mx + \frac{M}{2}\right) \quad \text{and} \quad M_2 = \left(Mx - \frac{M}{2}\right).$$

The variables Ψ, T and S in (2.7)–(2.9) are now written as a sum of mean (Ψ_0, T_0, S_0) and the perturbed quantities (ψ, θ, s). The perturbations are then considered to be proportional to $\exp[i\alpha z + \sigma\tau]$, where α is the wavenumber in the z direction and is a real quantity, and σ is the growth factor and is complex. The resulting linearized system of equations are

$$(d^2 - \alpha^2)^2 \psi - \frac{i\alpha}{Pr}\{W_0(d^2 - \alpha^2)\psi - \psi d^2 W_0\} + (R_t d\theta - R_s ds) - \frac{\sigma}{Pr}(d^2 - \alpha^2)\psi = 0, \tag{2.17}$$

$$(d^2 - \alpha^2)\theta + i\alpha\psi dT_0 - i\alpha W_0 \theta - \sigma\theta = 0, \tag{2.18}$$

$$Le(d^2 - \alpha^2)s + i\alpha\psi dS_0 - i\alpha W_0 s + d\psi - \sigma s = 0, \tag{2.19}$$

where

$$d = \frac{d}{dx} \quad \text{and} \quad \sigma = \sigma_r + i\sigma_i;$$

also

$$\psi = \Psi - \Psi_0, \quad \theta = T - T_0 \quad \text{and} \quad s = S - S_0.$$

The boundary conditions are

$$\psi = d\psi = \theta = ds = 0 \quad \text{at} \quad x = \pm \tfrac{1}{2}. \tag{2.20}$$

3. Method of solution

Following Chandrasekhar (1961), we expand the variables in (2.17)–(2.19) in terms of complete sets of orthogonal functions which satisfy the homogeneous boundary conditions in equation (2.20). We write

$$\psi = \sum_{j=1}^{\infty} a_j \psi_j, \tag{3.1}$$

$$\theta = \sum_{j=1}^{\infty} b_j \theta_j, \tag{3.2}$$

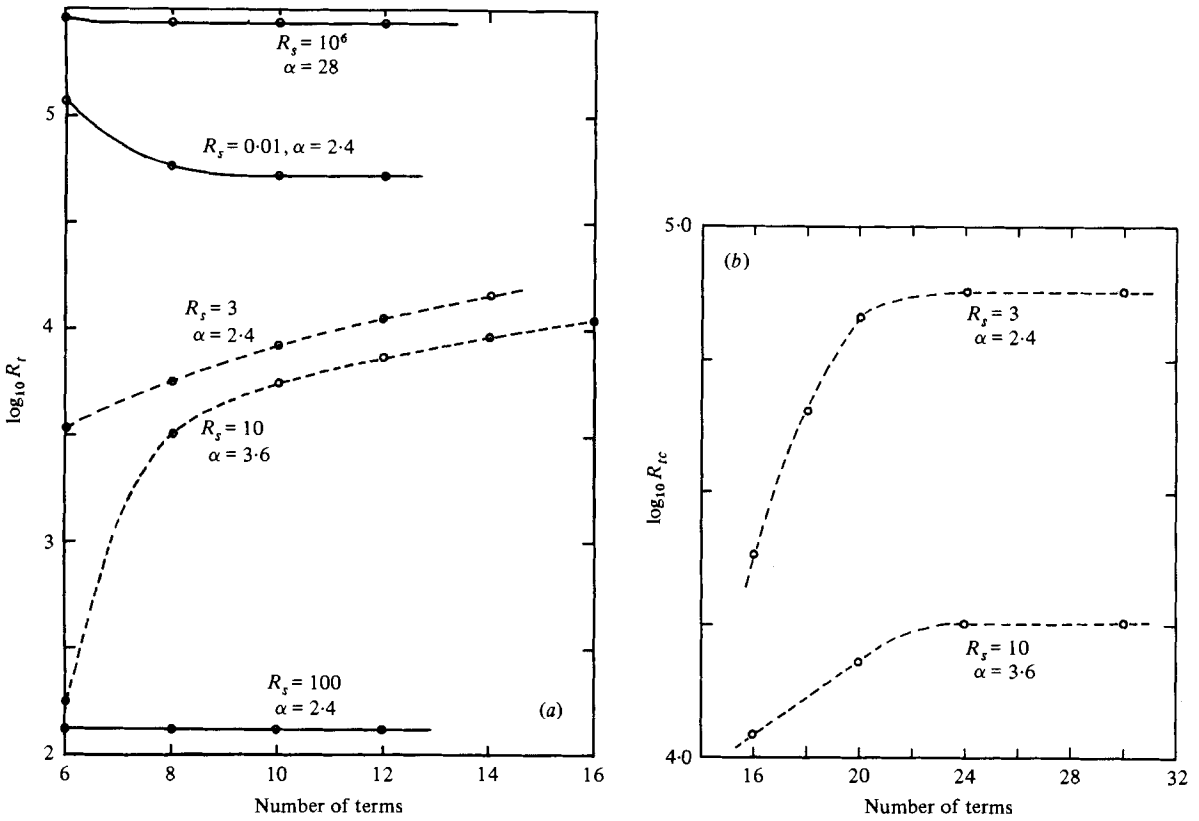

FIGURE 2. Evaluation of numerical convergence at different values of the solute Rayleigh number R_s. (*a*) Number of terms: 6–16. (*b*) Number of terms: 16–30. ---, overstable; ——, stationary.

$$s = \sum_{j=1}^{\infty} c_j s_j, \tag{3.3}$$

where

$$\psi_j = \begin{cases} \cosh(\mu_j x)/\cosh(\tfrac{1}{2}\mu_j) - \cos(\mu_j x)/\cos(\tfrac{1}{2}\mu_j) & \text{if } j \text{ is odd,} \\ \sinh(\mu_j x)/\sinh(\tfrac{1}{2}\mu_j) - \sin(\mu_j x)/\sin(\tfrac{1}{2}\mu_j) & \text{if } j \text{ is even,} \end{cases}$$

$$\theta_j = \begin{cases} \cos j\pi x & \text{if } j \text{ is odd,} \\ \sin j\pi x & \text{if } j \text{ is even,} \end{cases}$$

$$s_j = \begin{cases} \cos(j-1)\pi x & \text{if } j \text{ is odd,} \\ \sin(j-1)\pi x & \text{if } j \text{ is even,} \end{cases}$$

and μ_j are the zeros of

$$\tanh(\tfrac{1}{2}\mu_j) + \tan(\tfrac{1}{2}\mu_j) = 0 \quad \text{if } j \text{ is odd,}$$
$$\coth(\tfrac{1}{2}\mu_j) - \cot(\tfrac{1}{2}\mu_j) = 0 \quad \text{if } j \text{ is even.}$$

These functions have been successfully used by Paliwal & Chen (1980*b*). A Galerkin method is used to solve the resulting formal expressions, by making them orthogonal to the functions themselves. A linear system of homogeneous algebraic equations for the unknown coefficients are obtained and these may be written in the form of

$$(\mathbf{A} - \sigma \mathbf{I})\,\mathbf{x} = 0. \tag{3.4}$$

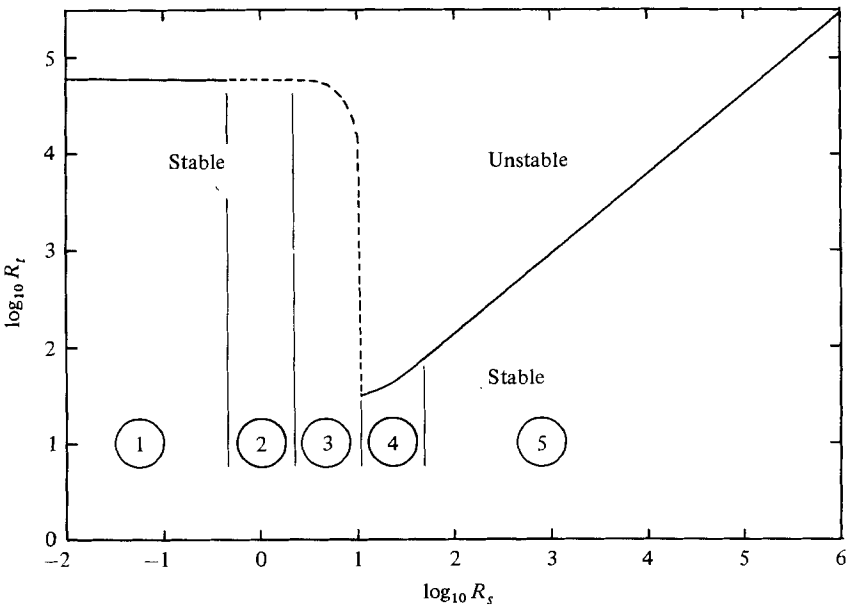

FIGURE 3. The neutral stability curve. $Pr = 6{\cdot}7$ and $Le = 1/101$. 1, $0 \leqslant R_s \leqslant 0{\cdot}45$; 2, $0{\cdot}45 < R_s < 3$; 3, $3 \leqslant R_s \leqslant 10$; 4, $10 < R_s \leqslant 60$; 5, $60 < R_s$. ---, overstable; ——, stationary.

The vector $\mathbf{x}$ contains the unknown coefficients a_j, b_j and c_j, and the matrix $\mathbf{I}$ is the identity matrix.

The system of equations (3.4) can be solved as a general eigenvalue problem and, since this is accomplished numerically, this infinite set of equations is first made finite by suitable truncation. The eigenvalues, σ, of this system of equations are then obtained by the modified LR algorithm of Martin & Wilkinson (1968*a*, *b*). In general, the eigenvalue σ is a function of the solute Rayleigh number, R_s, the thermal Rayleigh number, R_t, the wavenumber, α, the Prandtl number, Pr, and the Lewis number, Le. The neutral states of these parameters occur when the condition $\max\{\sigma_r\} = 0$ is satisfied, and these states are considered to be stationary, when the value of σ_i associated with $\max\{\sigma_r\}$ is zero, and overstable if it is non-zero (Chandrasekhar 1961). In this analysis, the Prandtl number and the Lewis number are held constant at 6·7 and 1/101 respectively. These values correspond to that of a typical heat–salt system. Thus, to obtain the neutral stability curves, any two of the three remaining parameters, R_s, R_t and α are kept constant and the third is varied until a neutral state is obtained.

The number of terms used in the expansions for computational purposes was determined based on an analysis for the numerical convergence of the results. Figures 2(*a*, *b*) show the change in the value of the thermal Rayleigh number at neutral conditions due to changes in the number of terms used in the expansions for different values of solute Rayleigh number, R_s. As shown in the figure, for values of R_s at 10^{-2}, 10^2 and 10^6 the results indicate very good convergence even with eight terms. However, at values of R_s of 3 and 10, satisfactory convergence could be obtained only with 24 terms. The results reported in the following were all computed with 12 terms, except when $3 \leqslant R_s \leqslant 10$, for which case 24 terms were used.

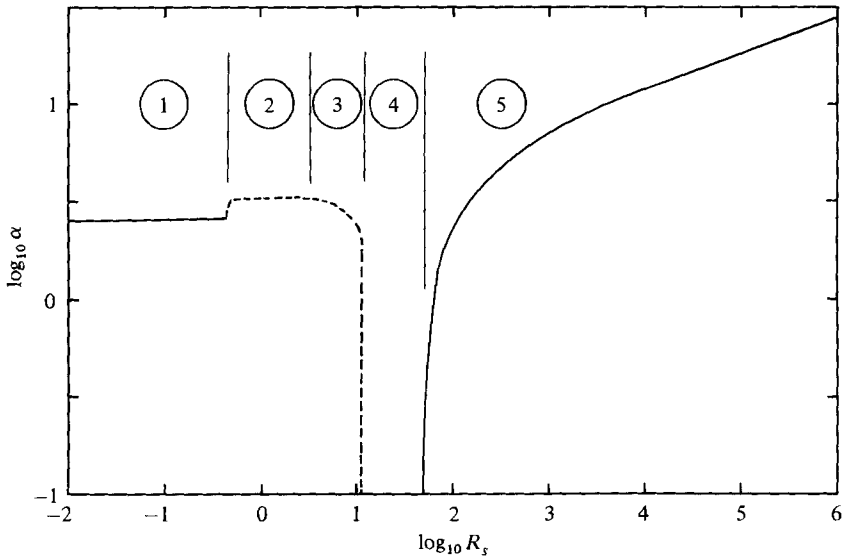

FIGURE 4. Critical wavenumber as a function of the solute Rayleigh number. Other details are same as shown in figure 3. ---, overstable; ——, stationary.

4. Results and discussion

The neutral stability curves are shown in figures 3 and 4. These curves are divided into five regions. In regions 1 and 5, the onset of instability is characterized by the formation of stationary two-dimensional rolls. As indicated by Hart (1970), in region 1 the instability is stationary, and is induced by the shear with the energy for the perturbations coming from the mean velocity field. In region 5, the instability is double-diffusive in nature, and the damping effect of the vertical stratification causes an increase in the critical wavenumber and the critical thermal Rayleigh number with an increase in the solute Rayleigh number.

In region, 2, however, we have shear instability with a sharp, but small, increase in the critical wavenumber. An increase in the value of R_s is associated with an increase in the lateral salinity gradient, and this gradient in essence provides the restoring force needed for the overstable motion but not strong enough to trigger the double-diffusive mechanism. The magnitude of mean shear in this region is still substantial when compared to that in regions 4 and 5 (see Hart 1971; Paliwal & Chen 1980*b*). The neutral stability curves at different values of solute Rayleigh number, R_s, corresponding to regions 1 and 2 are shown in figure 5. As can be seen, when the value of $R_s = 0{\cdot}1$, the neutral curve is stationary throughout the region indicated in the figure. For all other values of R_s, these curves are bimodal with stationary and overstable branches, and each with a separate and distinct minimum. The critical value, which is the smaller of these two minima, changes from stationary to overstable mode when the value of R_s changes from 0·3 to 0·4, marking the transition from region 1 to region 2 in the neutral curves indicated in figures 3 and 4.

In region 3, the destabilization is still shear induced. However, the stationary branches that characterize the neutral curves are absent in this region and the motion is overstable at the onset of instability. In addition, unlike that in region 2, the critical wavelength does not remain constant but increases with an increase in the value of R_s.

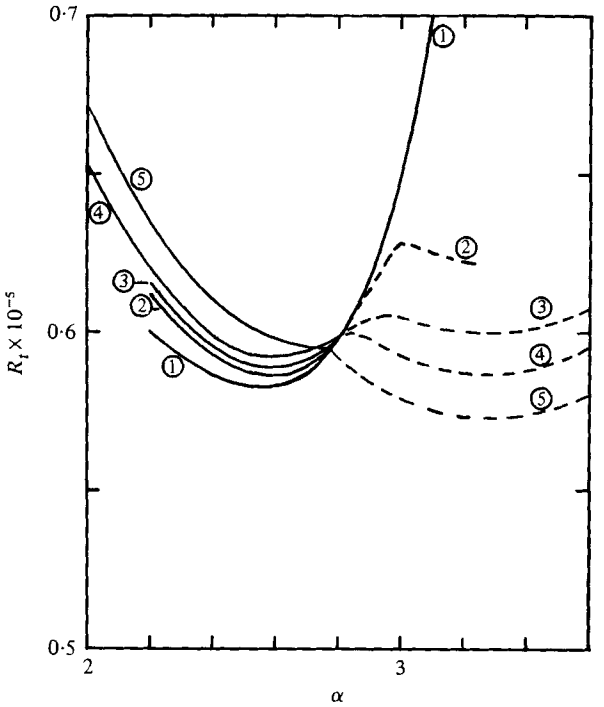

FIGURE 5. Thermal Rayleigh number as a function of wavenumber showing the transition from region 1 to region 2. – – –, overstable; ——, stationary. 1, $R_s = 0{\cdot}1$; 2, $R_s = 0{\cdot}3$; 3, $R_s = 0{\cdot}4$; 4, $R_s = 0{\cdot}5$; 5, $R_s = 10$.

In region 4, the destabilization occurs mainly due to the large difference in the equilibration times of heat and solute. Thus, the lateral motion of the fluid in the interior of the slot could create local sources of buoyancy causing instability. As shown in figure 3, the transition from the shear-induced, to the diffusive-type instability is very sharp with the critical value of the thermal Rayleigh number, R_{tc}, which changes from -10^4 to -30 when R_s changes from 10 to 11. This clearly shows that the temperature difference needed to destabilize a weak vertical solute gradient is, indeed, very small when the motion is driven by differential diffusion. Also it should be noted that the values of critical thermal Rayleigh number predicted here, are much smaller than those predicted by Hart (1970). This is mainly due to the fact that the corrections suggested by Paliwal & Chen (1980*b*) have been made in equation (3.3). Some neutral curves are shown in figure 7. As can be seen, for the value of R_s corresponding to region 4, there is no preferred wavelength at the critical state, indicating that the instability is not cellular in nature.

It is of interest to note here that, for the case of double-diffusive convection in a vertical layer of porous medium, saturated with stratified salt solution and subject to differential heating, similar conclusions were arrived at by Khan & Zebib (1981). In their analysis based on linear stability theory, they have shown that, for a finite range of values in R_s, the neutral curves become flat, and, although the value of R_{tc} is clearly defined in this region, there is no minimum value for the wavenumber. At values of R_s slightly larger than 60, the instability is cellular in nature with a preferred wavelength. This critical wavelength is quite large in the neighbourhood of the

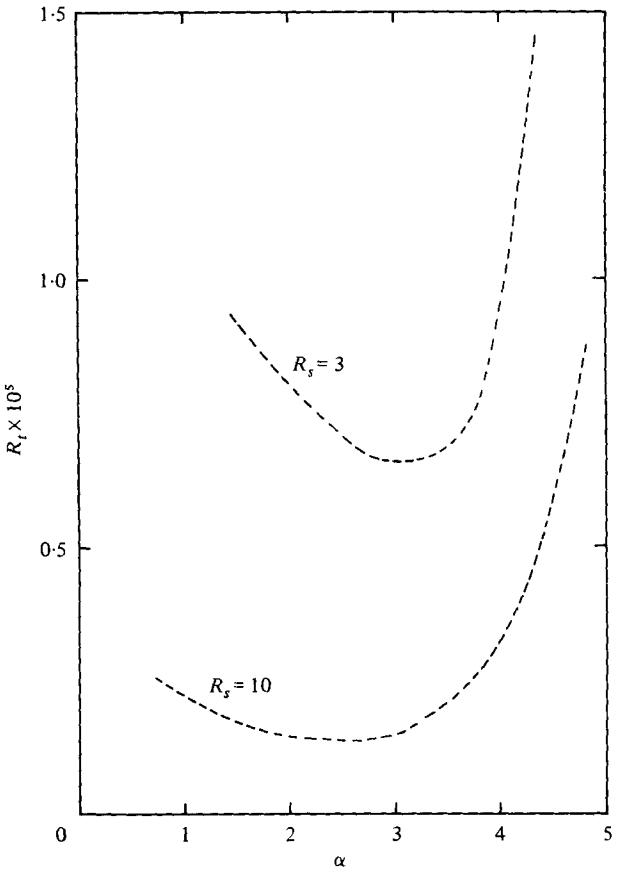

FIGURE 6. Thermal Rayleigh number as a function of wavenumber in region 3. -----, overstable.

transition from region 4 to 5. However, as the value of R_s increases further, the damping effect produced by the increase in the solute gradient in vertical direction becomes pronounced, resulting in the decrease of the critical wavelength.

5. Conclusions

In conclusion, we have shown that, during transition from purely thermal to thermo-solutal two-dimensional convection, the nature of the instability encountered is a strong function of the solutal Rayleigh number. As the value of R_s is increased from zero, the stationary shear-induced instability is replaced by an oscillatory shear instability. A further increase in R_s leads to stationary critical states without a preferred wavelength. This is followed by the doubly diffusive regime where the onset of instability is characterized by stationary two-dimensional cellular convection.

The authors would like to acknowledge the financial support provided by the National Science Foundation, through Grant ENG 78-16962.

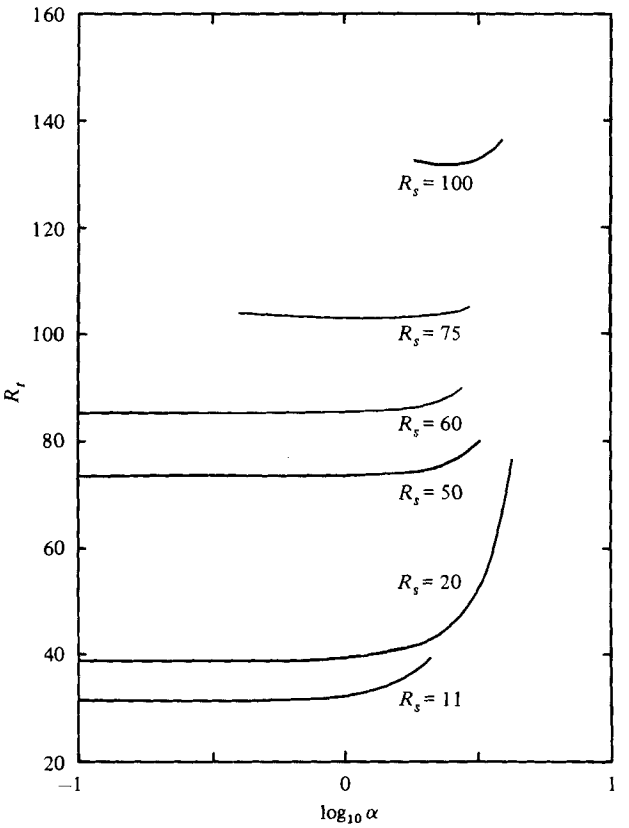

FIGURE 7. Thermal Rayleigh number as a function of wavenumber showing the transition from region 4 to region 5.

REFERENCES

CHANDRASEKHAR, S. 1961 *Hydrodynamic and Hydromagnetic Stability*. Clarendon Press.

ELDER, J. W. 1965 Laminar free convection in a vertical slot. *J. Fluid Mech.* **23**, 77–98.

HART, J. E. 1970 Thermal convection between sloping parallel boundaries. Ph.D. thesis, Massachusetts Institute of Technology.

HART, J. E. 1971 On sideways diffusive instability. *J. Fluid Mech.* **49**, 279–288.

KHAN, A. A. & ZEBIB, A. 1981 Double-diffusive instability in a vertical layer of porous medium. *J. Heat Transfer* **103**, 179–181.

MARTIN, R. S. & WILKINSON, J. H. 1968*a* Similarity reduction of a general matrix to Hessenberg form. *Numerische Mathematik* **12**, 349–368.

MARTIN, R. S. & WILKINSON, J. H. 1968*b* The modified LR algorithm for complex Hessenberg matrices. *Numerische Mathematik* **12**, 369–376.

PALIWAL, R. C. & CHEN, C. F. 1980*a* Double-diffusive instability in an inclined fluid layer. Part 1. Experimental investigations. *J. Fluid Mech.* **98**, 755-768.

PALIWAL, R. C. & CHEN, C. F. 1980*b* Double-diffusive instability in an inclined fluid layer. Part 2. Theoretical investigations. *J. Fluid Mech.* **98**, 769–785.

THORPE, S. A., HUTT, P. K. & SOULSBY, R. 1969 The effect of horizontal gradients on thermohaline convection. *J. Fluid Mech.* **38**, 375–400.